

## Preparation of TiO<sub>2</sub> rutile nanorods decorated with cobalt oxide nanoparticles for solar photoelectrochemical activity

Mathieu Grandcolas <sup>a\*</sup>, Brian Wabende <sup>a</sup>, Juan Yang <sup>a</sup>, Sen Mei <sup>a</sup>, Kaiqi Xu <sup>b</sup>, Truls Norby <sup>b</sup>, Athanasios Chatzitakis <sup>b</sup>

<sup>a</sup> SINTEF Industry, Department of Materials and Nanotechnology, Group of Nano and Hybrid Materials, Oslo, Norway

<sup>b</sup> University of Oslo, Department of Chemistry, Centre for Materials Science and Nanotechnology, Oslo, Norway

\* Corresponding author: mathieu.grandcolas@sintef.no

### Abstract

The present paper investigates the preparation of titanium dioxide (TiO<sub>2</sub>) nanorods decorated with cobalt oxide (Co<sub>3</sub>O<sub>4</sub>) nanoparticles and its application as solar photoelectrocatalyst. TiO<sub>2</sub> rutile nanorods have been prepared on conductive glass via a hydrothermal reaction in acidic media, shaped as squared rods with an average length of 1.7 μm and thicknesses between 50 and 120 nm. Co<sub>3</sub>O<sub>4</sub> nanoparticles with an average diameter of 30 nm were synthesized using a simple precipitation method. Spin coating the nanoparticles on the TiO<sub>2</sub> nanorods shows enhanced photocurrents under simulated solar light up to 1.3 mA/cm<sup>2</sup> at 1.6 V vs. SHE.

Keywords: Titania nanorods; Cobalt oxide; Photoanode; Nanoparticles; Solar energy materials; Photoelectrochemical cell

## Introduction

Photoelectrochemical (PEC) water splitting has attracted much attention as an environment friendly method for the production of green fuels [1]. Titanium dioxide ( $\text{TiO}_2$ ) is a material of choice that has been extensively studied as photoanode in PEC water splitting due to its low-cost, nontoxicity, and excellent physical and chemical stability [2]. However, the solar-to-hydrogen efficiency of  $\text{TiO}_2$  photoanodes is restricted by the wide band gap (3.0 - 3.2 eV), high recombination of the photogenerated carriers and sluggish water splitting kinetics [3]. In order to improve the PEC oxygen evolution reaction (OER), several semiconductors with co-catalysts have been investigated [4,5]. Among these, cobalt-based nanostructures have been reported to be very efficient OER co-catalysts on a variety of oxide semiconductors [6,7].

One-dimensional  $\text{TiO}_2$  nanomaterials have also shown unique structural and functional properties and have recently gain interest in hydrogen generating PEC cells [8]. Still, only a few publications have recently highlighted the potential of  $\text{TiO}_2$  nanotubes or nanorods with cobalt oxide for use of visible light or solar applications. Anodized vertically aligned  $\text{TiO}_2$  nanotubes coupled with cobalt-based oxides showed enhanced visible light effect on the photoelectrochemical performances of these materials [9,10,11]. Mishra *et al.* also proposed  $\text{TiO}_2/\text{Co}_3\text{O}_4$  core-shell nanorods as an efficient energy storage and electrochromic material [12]. Ramakrishnan et al. investigated  $\text{TiO}_2$  nanorods/FTO sensitized with cobalt oxide nanoparticles by electrochemical deposition, followed by rapid thermal annealing under air and  $\text{N}_2$ , and showed improved PEC properties [13].

In this work, we demonstrate an alternative simple spin coating method to decorate  $\text{TiO}_2$  nanorods with cobalt oxide nanoparticles towards simulated solar light PEC activity.

## Experimental

Preparation of samples:

The growth of  $\text{TiO}_2$  nanorods ( $\text{TiO}_2$  NRs) on FTO glass was performed by following a published procedure [14] with small modifications. 30 mL of deionized water was mixed with 30 mL concentrated

hydrochloric acid (37%) for 5 min in a Teflon-lined stainless-steel autoclave. Then, 1 mL of titanium butoxide was added and mixed for 5 min. Fluorine doped tin oxide (FTO) glasses (Dyesol TEC15) were laser cut in size 5 x 2.5 cm and ultrasonically cleaned for 5 min in a beaker using acetone, isopropanol, ethanol and water, successively. One cleaned FTO glass was placed at an angle against the wall of the Teflon liner with the conducting side facing down. The hydrothermal synthesis was conducted at 150 °C for 6 h in a heating cabinet. The FTO glass were then thoroughly rinsed with distilled water and dried at 90 °C.

Cobalt oxide nanoparticles were synthesized by a precipitation method. 5 g of cobalt nitrate ( $\text{Co}(\text{NO}_3)_2$ ) and 14.7 g tetraethylammonium hydroxide (TENOH) were dissolved in 175 mL water and heat treated at 80 °C for 6 h under agitation. The suspension was then washed 3 times with water using centrifugation and redispersed to obtain a 0.1 wt% suspension.

$\text{TiO}_2$  nanorods decorated with cobalt oxide nanoparticles samples ( $\text{TiO}_2$  NRs +  $\text{Co}_3\text{O}_4$ ) were obtained by spin coating 200  $\mu\text{L}$  of the prepared cobalt oxide nanoparticles suspension on  $\text{TiO}_2$  nanorods/FTO at 3000 rpm for 30s.

#### Characterizations:

Morphology of the samples was observed with scanning electron microscopy (SEM) using a FEI Nova NanoSEM 650 FEG-SEM microscope. Transmission electron microscopy (TEM) was used to observe cobalt oxide nanoparticles using a JEOL 2010F operating at 200 kV. The crystalline phase of the samples was determined by X-ray diffraction (XRD) in a Bruker D8 Discover diffractometer using  $\text{Cu K}\alpha$ -filtered radiation.

The photoelectrochemical characterization was performed in an in-house made three-electrode electrochemical cell equipped with a quartz window. A 200W Newport Xenon-mercury lamp equipped with an air mass 1.5G mass filter was used. The lamp was placed at a distance from the electrode's surface so that 1 Sun ( $100 \text{ mW}/\text{cm}^2$ ) could be detected with a calibrated reference Si PV cell (Newport, model 91150V). Pt foil and Ag/AgCl were used as counter and reference electrodes, respectively. The

electrolyte was a 0.5 M Na<sub>2</sub>SO<sub>4</sub> solution (pH 7.2). The applied potential and related measurements were obtained using a Gamry Reference 600 potentiostat. The reported potentials are calculated vs. the standard hydrogen electrode (SHE) using Eq. 1:

$$E_{\text{SHE}} = E_{\text{Ag/AgCl}} + 0.059\text{pH} + E_{\text{Ag/AgCl}}^0 = E_{\text{Ag/AgCl}} + 0.401 + 0.197 = E_{\text{Ag/AgCl}} + 0.598 \quad \text{Eq. 1}$$

## Results and discussion

TiO<sub>2</sub> nanorods were grown on FTO glass substrates using a modified one-pot hydrothermal synthesis as previously reported [14]. A typical top-view SEM image of a TiO<sub>2</sub> NRs film grown for 6h on FTO is shown in Figure 1b. We observed a densely packed array of vertically aligned TiO<sub>2</sub> NRs, appearing as tetragonal in shape with an average diagonal length ranging between 50 and 120 nm, and with an average length estimated around 1.7 μm (see also S1). The top surface of the nanorods contains many step edges, while the side surface is smooth, as previously observed [14]. Cobalt oxide nanoparticles were prepared via a precipitation method and TEM analysis showed a homogeneous distribution of particles sizes in the range 20-40 nm (Figure 1a). Figure 1c shows the TiO<sub>2</sub> NRs sample with the addition of cobalt oxide nanoparticles, which appear to be attached mostly at the edged top surfaces rather than at the sides of the TiO<sub>2</sub> NRs (see also S1). The density of the NRs is rather high and the Co<sub>3</sub>O<sub>4</sub> nanoparticles appear mainly at the top of the NRs.

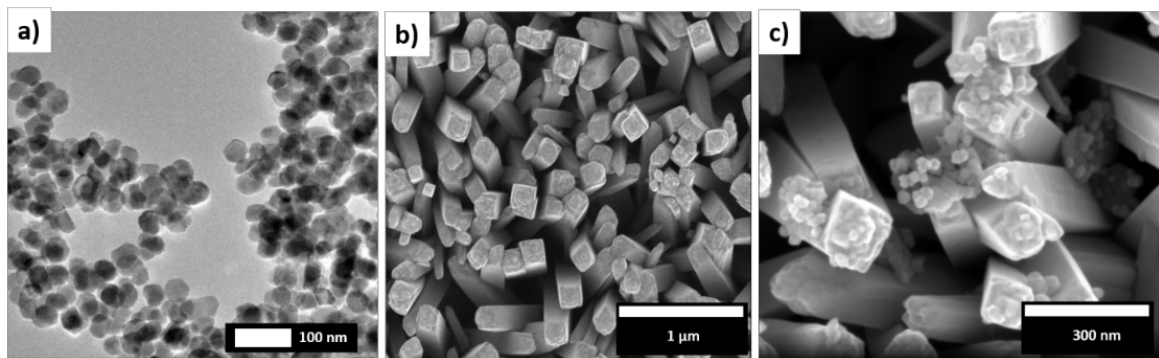


**Figure 1:** (a) TEM picture of Co<sub>3</sub>O<sub>4</sub> nanoparticles, (b) SEM of TiO<sub>2</sub> NRs on FTO and (c) SEM of TiO<sub>2</sub> NRs + Co<sub>3</sub>O<sub>4</sub> nanoparticles

Figure 2 shows the XRD pattern of the cobalt oxide nanoparticles obtained after the chemical precipitation process. The diffraction pattern of the obtained powder was indexed to the crystalline

phase of cobalt oxide  $\text{Co}_3\text{O}_4$  [15]. Figure 2 shows the XRD patterns of  $\text{TiO}_2$  NRs on FTO. The sample exhibited XRD patterns ascribed to tetragonal rutile and several peaks corresponding to the underneath FTO glass. For the sample  $\text{TiO}_2$  NRs +  $\text{Co}_3\text{O}_4$  we could not detect any peaks corresponding to the crystalline phase of  $\text{Co}_3\text{O}_4$  within the detection limits of XRD, probably due to the low concentration of nanoparticles on the surface of the sample and some peak overlapping.

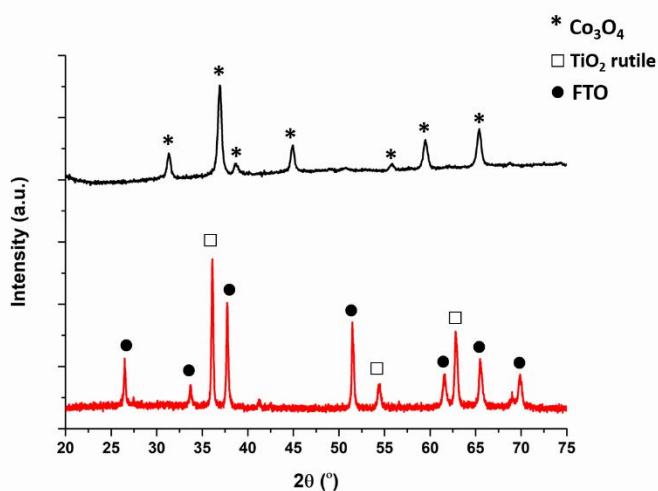


**Figure 2:** XRD patterns of Cobalt oxide nanoparticles (up, black) and  $\text{TiO}_2$  nanorods on FTO (down, red).

Figure 3a shows the linear sweep voltammetry (LSV) curves of the  $\text{TiO}_2$  NRs and  $\text{TiO}_2$  NRs +  $\text{Co}_3\text{O}_4$  photoanodes, under  $100 \text{ mW/cm}^2$  simulated solar illumination and dark conditions. A low current ( $< 50 \mu\text{A/cm}^2$ ) is measured in dark conditions under the whole potential scan area for both samples. On the contrary, at a fixed potential of *i.e.* **1.6 V vs. SHE** under illumination, the  $\text{TiO}_2$  NRs sample shows a photocurrent density of  $0.7 \text{ mA/cm}^2$ , while for the sample of  $\text{TiO}_2$  NRs +  $\text{Co}_3\text{O}_4$  nanoparticles the photocurrent density almost doubles and reaches up to  $1.3 \text{ mA/cm}^2$ . Figure 3b depicts the chronoamperometry (CA) curve of the same photoanodes under chopped light irradiation at **0.6 V, 1.2 V and 1.6 V vs. SHE**. The photocurrent densities in the CA experiments are in agreement with the LSV measurements, which imply that the scanning rate of  $10 \text{ mV/s}$  was sufficiently low to reach steady-state conditions. The photoconversion efficiency (PE) is given in Figure S2.

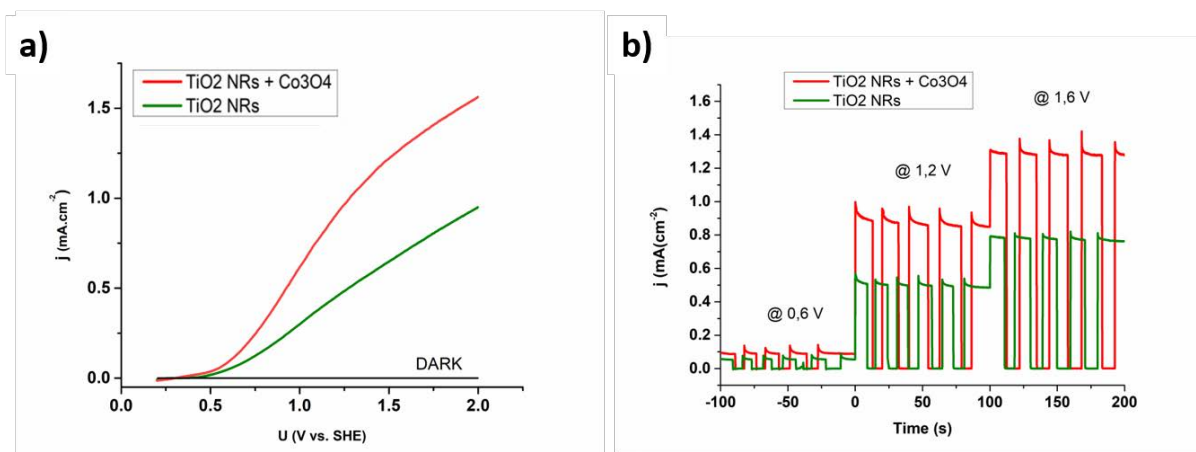


**Figure 3:** LSV at a scan rate of 10 mV/s (a) and CA (b) of TiO<sub>2</sub> NRs and TiO<sub>2</sub> NRs + Co<sub>3</sub>O<sub>4</sub>

The net increase of the photocurrent response is mainly attributed to the improvement of the water splitting kinetics due to the presence of the Co<sub>3</sub>O<sub>4</sub> electrocatalyst. Although Co<sub>3</sub>O<sub>4</sub> is a p-type semiconductor with an indirect band gap generally found in the region of 1.6–2.2 eV [16], a film of Co<sub>3</sub>O<sub>4</sub> on FTO glass is photoelectrochemically inactive under 1 sun simulated light (Fig. S3). On the other hand, electrochemical impedance spectroscopy (EIS) measurements highlight the blocking and interfacial charge transfer behaviour in the dark and under illumination, respectively (Fig. S4). Especially, under light conditions, the Co<sub>3</sub>O<sub>4</sub> modified electrode shows a lower interfacial charge transfer resistance, as indicated by the smaller semicircle in the intermediate to low frequency range of the Nyquist plot (S4 inset). The heterojunction between Co<sub>3</sub>O<sub>4</sub> and TiO<sub>2</sub> can efficiently promote charge separation and inhibit recombination of photogenerated electron-hole pairs in the TiO<sub>2</sub> nanostructure. Ramakrishnan *et al.* [13] described the phenomenon where photogenerated electrons move from the conduction band of cobalt oxide to that of TiO<sub>2</sub> and then to the FTO substrate for the photoelectrochemical reaction to occur. Hole movement occurs in the reverse direction towards the interface with the electrolyte, oxidizing adsorbed water molecules, and the overall formed system enhances the photocatalytic properties of the photoanode. Lastly, the stability of TiO<sub>2</sub> NRs + Co<sub>3</sub>O<sub>4</sub> was assessed for 180 min of operation under simulated light at 1.2 V vs. SHE (Fig. S5) and show excellent stability with no degradation.

## Conclusion

TiO<sub>2</sub> nanorods films show potential for application in PEC technologies. It was observed that the addition of an oxygen evolution reaction catalyst like cobalt oxide Co<sub>3</sub>O<sub>4</sub> enhances significantly the photocurrent response under simulated solar light. In this work we prepared TiO<sub>2</sub> nanorods on FTO glass, decorated them with Co<sub>3</sub>O<sub>4</sub> by a simple spin-coating and showed that we could nearly double the amount of photocurrent generated under simulated solar light with a maximum of 1.3 mA/cm<sup>2</sup> at 1.6 V vs. SHE.

## Acknowledgement

This work has been funded by the Research Council of Norway under the NANO2021 program, project CO2BioPEC (250261).

## References

- 
- [1] C. Jiang, S.J. Moniz, A. Wang, T. Zhang, J. Tang, *Chem. Soc. Rev.* 46 (2017) 4645-4660
  - [2] M. Humayun, F. Raziq, A. Khan, W. Luo, *Green Chem. Lett. Rev.* 11 (2018) 86-102
  - [3] O. Khaselev, J.A. Turner, *Science* 280 (1998) 425-427
  - [4] J. Yang, D. Wang, H. Han and C. Li, *Acc. Chem. Res.*, 46 (2013) 1900–1909
  - [5] L. Yang, H. Zhou, T. Fan and D. Zhang, *Phys. Chem. Chem. Phys.*, 16 (2014) 6810–6826.
  - [6] M.A. Khan, M. Al-Oufi, S. Tossef, Y. Al-Salik, H. Idriss, *Catalysis, Structure & Reactivity* 1 (2015) 192-200
  - [7] K. Xu, A. Chatzidakis, I.J.T. Jensen, M. Grandcolas, T. Norby, *Photochem. Photobiol. Sci.*, 2019, Advance Article, DOI: 10.1039/C8PP00312B
  - [8] M. Ge, C. Cao, J. Huang, S. Li, Z. Chen, K.-Q. Zhang, S.S. Al-Deyab, Y. Lai, *J. Mater. Chem. A* 4 (2016) 6772-6801
  - [9] H. Ali, N. Ismail, M. Mekewi, A.C. Hengazy, *J. Solid State Electrochem.* 19 (2015) 3019-30-26

- 
- [10] B. Huang, W. Yang, Y. Wen, B. Shan, R. Chen, *Appl. Mater. Interfaces* 7 (2015) 422-431
- [11] S. Qarechalloo, N. Naseri, F. Salehi, A.Z. Moshfegh, *Appl. Surf. Sci.* 464 (2019) 68-77
- [12] S. Mishra, P. Yogi, P.R. Sagdeo, R. Kumar, *ACS Appl. Energy Mater.* 1 (2018) 790-798
- [13] V. Ramakrishnan, H. Kim, J. Park, B. Yang, *RSC Adv.* 6 (2016) 9789-9795
- [14] B. Liu, S. Aydil, *J. Am. Chem. Soc.* 131 (2009) 3985-3990
- [15] C. Feng, H. Wang, J. Zhang, W. Hu, Z. Zou, Y. Deng, *J. Nanopart. Res.* 16 (2014) 2413-2423
- [16] J.M. Xu, J.P. Cheng, *J. Alloys Compounds* 686 (2016) 753-768



# Supporting Information

**Preparation of TiO<sub>2</sub> rutile nanorods decorated with cobalt oxide nanoparticles for solar photoelectrochemical activity**

Mathieu Grandcolas <sup>a\*</sup>, Brian Wabende <sup>a</sup>, Juan Yang <sup>a</sup>, Sen Mei <sup>a</sup>, Kaiqi Xu <sup>b</sup>, Truls Norby <sup>b</sup>, Athanasios Chatzitakis <sup>b</sup>

<sup>a</sup> SINTEF Industry, Department of Materials and Nanotechnology, Group of Nano and Hybrid Materials, Oslo, Norway

<sup>b</sup> University of Oslo, Department of Chemistry, Centre for Materials Science and Nanotechnology, Oslo, Norway

\* Corresponding author: [mathieu.grandcolas@sintef.no](mailto:mathieu.grandcolas@sintef.no)

Cross section SEM image

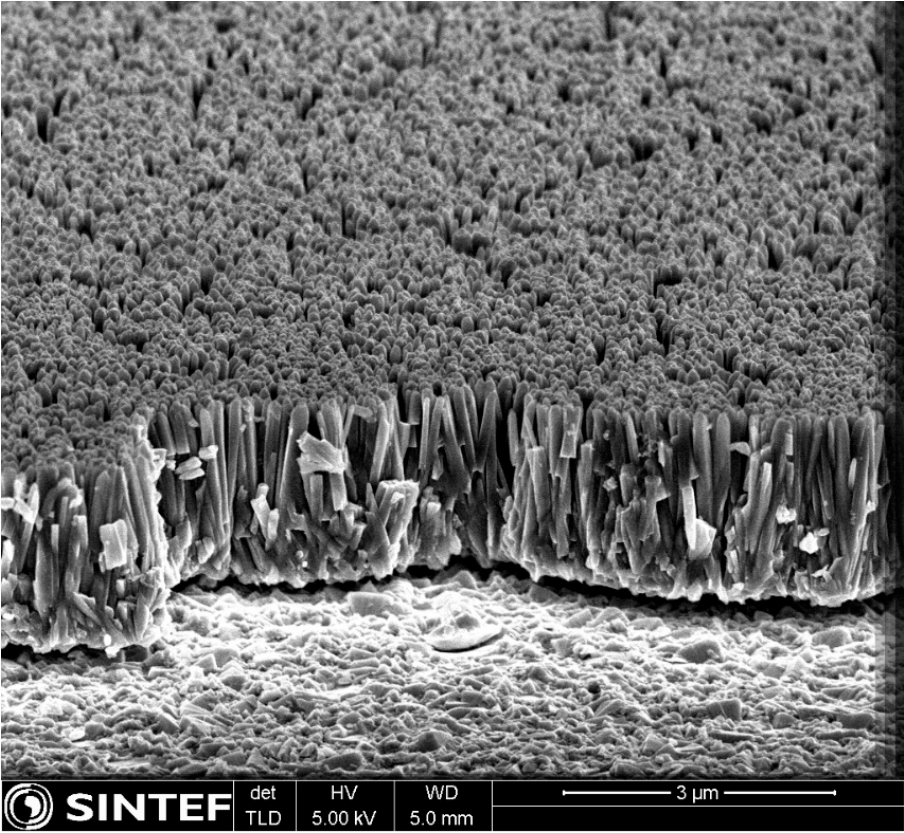


Figure S1: Cross section SEM image of the TiO<sub>2</sub> NRs + Co<sub>3</sub>O<sub>4</sub> photoelectrode

## Photoconversion efficiency

The photoconversion efficiency was calculated according to the following equation:

$$\eta = j_p \left( \frac{U_{rev}^0 - U_{app}}{I_0} \right) \times 100$$

where  $j_p$  is in mA/cm<sup>2</sup>,  $U_{rev}^0$  is the standard reversible potential for water splitting (1.23 V vs. SHE),  $U_{app}$  is the applied external potential vs. SHE, and  $I_0$  is the wavelength dependent intensity of incident light in mW/cm<sup>2</sup> [1].

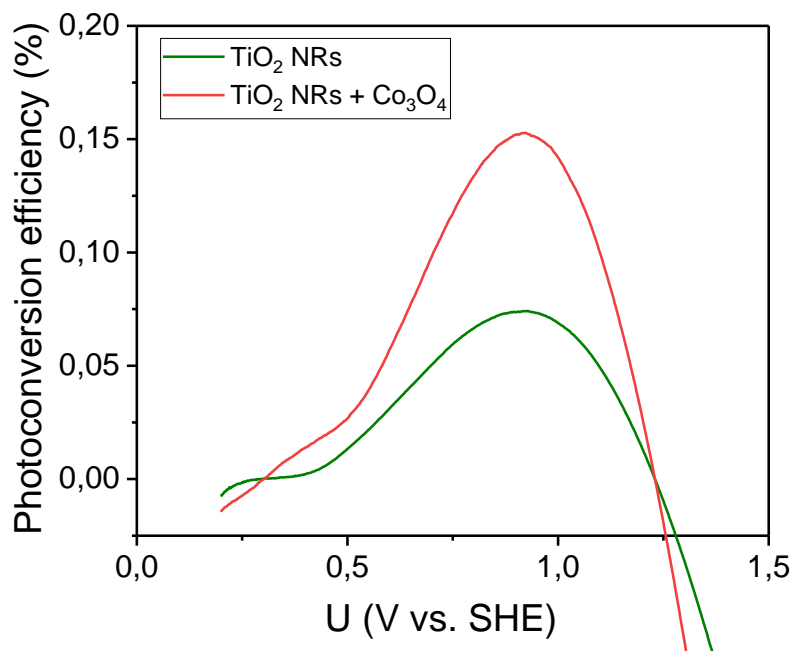


**Figure S2:** Photoconversion efficiency as a function of the applied potential

In both photoelectrodes the maximum PE is at approx. 0.9 V vs. SHE, and further increase in the applied potential (*i.e.* energy input) is not compensated by the increase in the photocurrent density, therefore PE decreases abruptly. Furthermore, the TiO<sub>2</sub> NRs + Co<sub>3</sub>O<sub>4</sub> exhibits double PE than the TiO<sub>2</sub> NRs, indicating the improved charge separation due to the presence of the electrocatalyst.

## LSV of $\text{Co}_3\text{O}_4$ on ITO

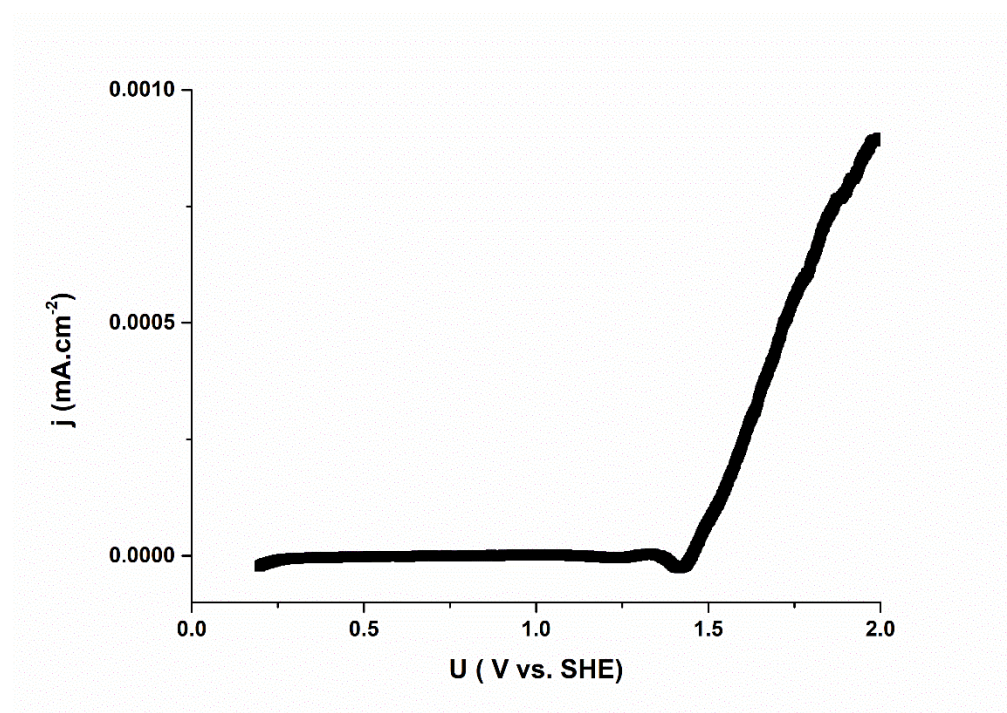


**Figure S3:** LSV at a scan rate of 10 mV/s of  $\text{Co}_3\text{O}_4$  nanoparticles spin coated on FTO under 1 sun simulated illumination

## Electrochemical impedance spectroscopy

EIS was recorded at a frequency range of 100 kHz to 100 mHz and the amplitude of the sinusoidal voltage was 10 mV RMS. The EIS was carried out at 1.2 V vs. SHE.

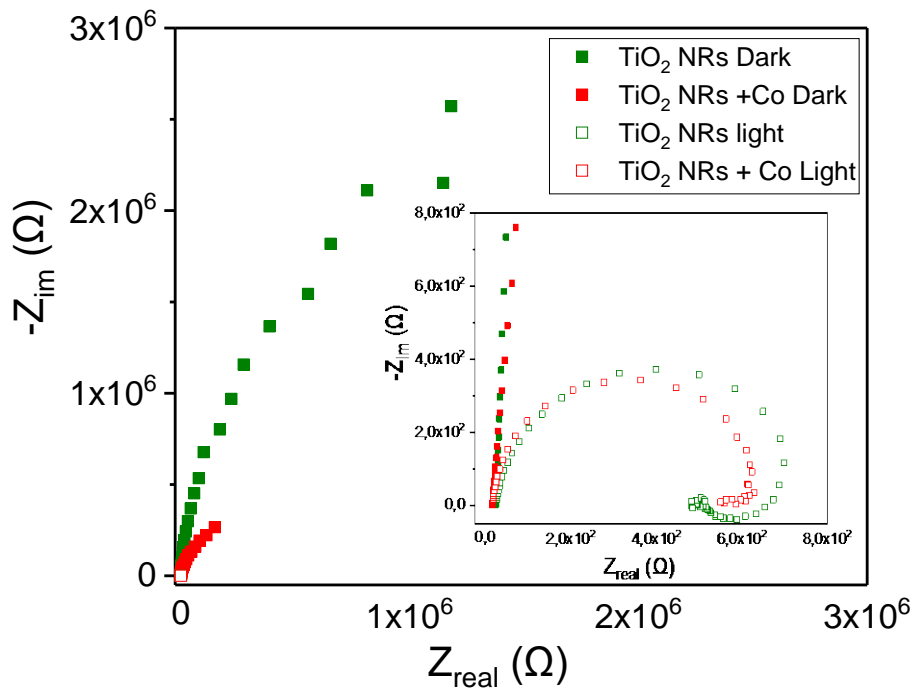


**Figure S4:** Nyquist plot of the  $\text{TiO}_2$  TNRs and  $\text{TiO}_2$  TNRs +  $\text{Co}_3\text{O}_4$  photoelectrodes in the dark (coloured squares) and under 1 sun illumination (empty squares) at 1.2 V vs. SHE. Inset: Zoom in at low real and imaginary resistances

## Stability test

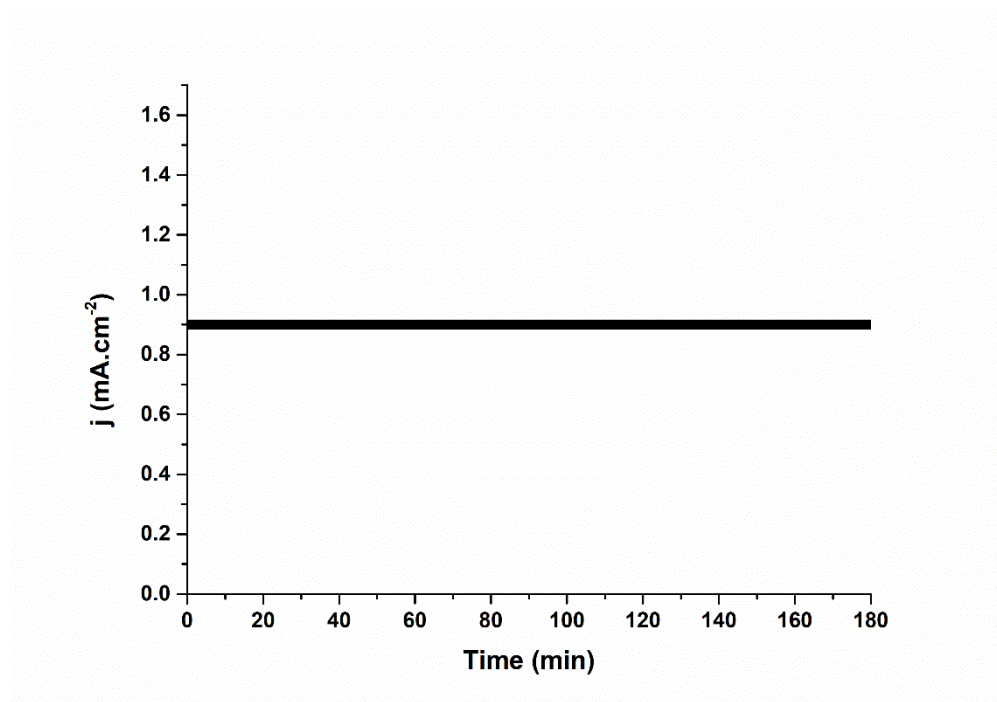


**Figure S5:** Stability test of  $\text{TiO}_2 + \text{Co}_3\text{O}_4$  over 180 min under 1 sun simulated light at 1.2 V vs. SHE.

## References

[1] Roel van de Krol, M. Grätzel, Photoelectrochemical Hydrogen Production, Springer US2012.